

## MICROSTRUCTURE ANALYSIS OF SYNTHESIZED LiBOB

Etty Marti Wigayati\*, Christin Rina Ratri, Ibrahim Purawiardi,  
Fadli Rohman, and Titik LestariningsihResearch Center for Physics, Indonesian Institute of Sciences, Kawasan Puspiptek Serpong Gd. 442  
Tangerang Selatan 15314, Banten Indonesia

Received March 3, 2015; Accepted June 4, 2015

## ABSTRACT

Lithium bis (oxalate) borate or LiBOB is an active material used as the electrolyte for lithium battery application. LiBOB ( $\text{LiB}(\text{C}_2\text{O}_4)_2$ ) powder was prepared from LiOH,  $\text{H}_2\text{C}_2\text{O}_4$  and  $\text{H}_3\text{BO}_3$ . The employed method was solid state reaction. LiBOB powder produced from the reaction was then observed using SEM and TEM. Surface area was analyzed using Quantachrome Nova 4200e. From the analysis analyzed using XRD to identify the resulting phases, crystal structure, and crystallite size. The functional groups were analyzed using FT-IR. The particle morphology was result, it was seen that the resulted phases were  $\text{C}_4\text{LiBO}_8$  and  $\text{LiB}(\text{C}_2\text{O}_4)_2 \cdot \text{H}_2\text{O}$ , the crystal structure was orthorhombic with space group *Pbca* and *Pnma*. From the particle morphology observation it was shown that micro pores were created irregularly. When the observation was deepened, nanopores with elongated round shape were seen within the micropores. The pore size was approximately 50–100 nm. The surface area, total pore volume, and average pore diameter of LiBOB powder was  $88.556 \text{ m}^2/\text{g}$ ,  $0.4252 \text{ cm}^3/\text{g}$ , and 19.2 nm respectively.

**Keywords:** phase; crystal structure; crystallite size; functional group; nanopores particle morphology

## ABSTRAK

LiBOB (Lithium bis oksalat borat) merupakan bahan aktif yang dapat dipergunakan untuk elektrolit pada baterai Lithium. Serbuk LiBOB ( $\text{LiB}(\text{C}_2\text{O}_4)_2$ ) dibuat dari bahan baku LiOH,  $\text{H}_2\text{C}_2\text{O}_4$  dan  $\text{H}_3\text{BO}_3$ . Metoda yang dipergunakan adalah solid state reaction. Serbuk LiBOB yang dihasilkan dianalisa menggunakan XRD untuk mengetahui fasa yang terbentuk, struktur kristal dan ukuran kristalinitasnya. Ikatan gugus fungsi dianalisa dengan FTIR. Morfologi partikel diamati dengan SEM dan TEM. Surface area dianalisis dengan alat Quantachrome Nova 4200e. Dari hasil analisis dapat diketahui bahwa fasa yang terbentuk adalah fasa  $\text{C}_4\text{LiBO}_8$  dan  $\text{LiB}(\text{C}_2\text{O}_4)_2(\text{H}_2\text{O})$ , struktur kristal orthorhombic dengan space group *Pbca* dan *Pnma*. Pada pengamatan morfologi partikel dapat diketahui terbentuk rongga pori dalam ukuran mikro dengan bentuk tidak beraturan. Ketika pengamatan diperdalam lagi pada bagian rongga pori nampak terjadi nanopori dengan bentuk bulat sedikit memanjang. Ukuran pori berkisar 50-100 nm. Luas permukaan, volume pori total, dan rerata diameter pori dari serbuk LiBOB masing-masing adalah  $88,556 \text{ m}^2/\text{g}$ ,  $0,4252 \text{ cm}^3/\text{g}$ , dan 19,2 nm.

**Kata Kunci:** fasa; struktur kristal; ukuran kristalinit; ikatan gugus; morfologi partikel nanopori

## INTRODUCTION

Lithium bis(oxalato) borate (LiBOB) is a new lithium salt firstly proposed at 1999 by Lischka et al. [1-2] as a highly promising and advantageous electrolyte for rechargeable lithium-ion batteries. Thermal behavior of LiBOB is an interesting and important research subject especially concerning the safety of lithium-ion batteries. In the last few years, several researchers have published LiBOB-related scientific journals, particularly discussing thermal studies of LiBOB which showed excellent thermal stability up to 300 °C. Beyond this temperature, LiBOB would be decomposed into  $\text{Li}_2\text{CO}_3$ ,  $\text{B}_2\text{O}_3$ , and  $\text{CO}_2$  [3-5]. Another publication explained that LiBOB electrolyte dissolved in propylene carbonate (PC)

solvent that showed has higher power capability compared to another lithium salts in similar solvent [6-7]. It was also explained that the charge/discharge test of 0.7 M LiBOB in EC:EMC (1:1) solvent showed more superior performance compared to 1 M  $\text{LiPF}_6$  in EC:EMC (1:1) solvent. LiBOB has higher stability and discharge capacity at high temperature [8].

In addition, LiBOB has distinctive physical properties such as hygroscopic and stable when it contacts with water. However, LiBOB solubility in the mixture of carbonate solvent to form liquid electrolyte was found to be relatively low compared to  $\text{LiPF}_6$ , therefore microstructure observation of LiBOB powder is necessary. In this research, LiBOB powder was synthesized using solid state reaction method, and

\* Corresponding author. Tel/Fax : +62-21-7560570/7560556  
Email address : etty001@lpi.go.id

microstructure analysis was performed to observe the pores. Produced crystal structure space group, crystallite size, and cell density were analyzed using X-Ray Diffraction (XRD), and the functional groups using Fourier Transform Infra Red (FT-IR) spectroscopy.

## EXPERIMENTAL SECTION

### Materials

The materials used in this research were oxalic acid ( $\text{H}_2\text{C}_2\text{O}_4 \cdot 2\text{H}_2\text{O}$ ) with 98% purity, lithium hydroxide (LiOH) with 98% purity, and boric acid ( $\text{H}_3\text{BO}_3$ ) with 98% purity. All materials were supplied from Merck (Germany).

### Instrumentation

The heat treatment for preparing LiBOB was performed using Thermolyne muffle furnace. Crystalline structure and the crystallinity of the powder were analysed using X-Ray Diffractometer (XRD) Rigaku type SmartLab. The functional groups were analyzed using FT-IR Thermoscientific type Nicolet iS-10 machine. The surface morphology of LiBOB powder, characterization using Scanning Electron Microscope (SEM) Hitachi SU-3500 and Transmission Electron Microscope (TEM) FEI type Tecnai G<sup>2</sup> 20S-Twin 200 kV acceleration voltages. Surface area of LiBOB powder was observed using Quantachrome Nova 4200e.

### Procedure

To synthesize LiBOB, solid state reaction among oxalic acid, lithium hydroxide, and boric acid was performed with chemical reaction scheme as follows [9]:  

$$2\text{H}_2\text{C}_2\text{O}_4 \cdot 2\text{H}_2\text{O} + \text{LiOH} \cdot \text{H}_2\text{O} + \text{H}_3\text{BO}_3 \rightarrow \text{LiB}(\text{C}_2\text{O}_4)_2 + 9 \text{H}_2\text{O}$$

Reactants used for synthesizing LiBOB are lithium hydroxide, boric acid, and oxalic acid. These materials were pre-treated first to remove moisture. Reactants were weighed and mixed following molar ratio of 2:1:1. Heating process was performed in a muffle furnace at 120 °C temperature for 4 h and 240 °C for 6 h, subsequently. The product obtained from the heating was white powder.

### X-Ray diffraction

Powder crystallinity of the LiBOB sample was scanned using X-Ray Diffractometer (XRD) with CuK $\alpha$  target, wave length  $\lambda = 1.5406 \text{ \AA}$ , and  $2\theta$  range of 10° to 80°. A diffractogram with diffraction peaks was obtained as a result; that was analysed with PDXL software to collect formed phase information as well as qualitative analysis including crystal structure parameter in a unit

cell and space group. The degree of crystallinity was calculated empirically using the following formula [10]:

$$\chi_c (\%) = \frac{A_c}{A_c + A_a} \times 100\%$$

$A_c$  = area of crystalline region,  $A_a$  = area of amorphous region, and  $\chi_c$  = degree of crystallinity.

### FT-IR spectroscopy

Fourier Transform Infra Red (FT-IR) spectroscopy of LiBOB powder was obtained to identify the functional groups. FT-IR spectroscopy scanning was conducted within wavenumber range of 4000 to 600  $\text{cm}^{-1}$  with ATR method.

### Scanning and Transmission Electron Microscopy (SEM and TEM)

To identify the surface morphology of LiBOB powder, characterization using SEM was performed. The sample was prepared by putting it onto carbon tape and coating it with pure gold (Au) using sputter-coating method to increase specimen conductivity. To explore the surface morphology of the sample, Transmission Electron Microscope (TEM) was used. The sample was prepared by dispersing the powder with toluene in order to aid the attachment of the powder onto the surface of the grid, since the sample size on the grid was limited to be smaller than 200 nm. Toluene-dispersed sample was dropped on the grid using a pipette under an optical microscope. The prepared sample was then inserted into the TEM holder to be analyzed.

### Surface area analysis

Surface area of LiBOB powder was observed using surface area pore size analyzer, with Brunauer-Emmett-Teller (BET) method. In principle, this equipment employs gas (usually nitrogen) adsorption on the surface of a solid material which was characterized at a constant temperature (the boiling point of the gas). If the specific gas volume adsorbed on the surface of a solid material at a certain temperature and pressure is known, the theoretical surface area of one molecule of adsorbed and so the surface area of the solid material can be calculated. Total pore volume and average pore radius were also observed in this analysis.

## RESULT AND DISCUSSION

The X-ray diffraction pattern of LiBOB powder was presented in Fig. 1. Before analyzing the X-ray diffraction pattern, the phase from this pattern has to be found first. The important parameter to determine a phase is d-spacing value. Each phase has three

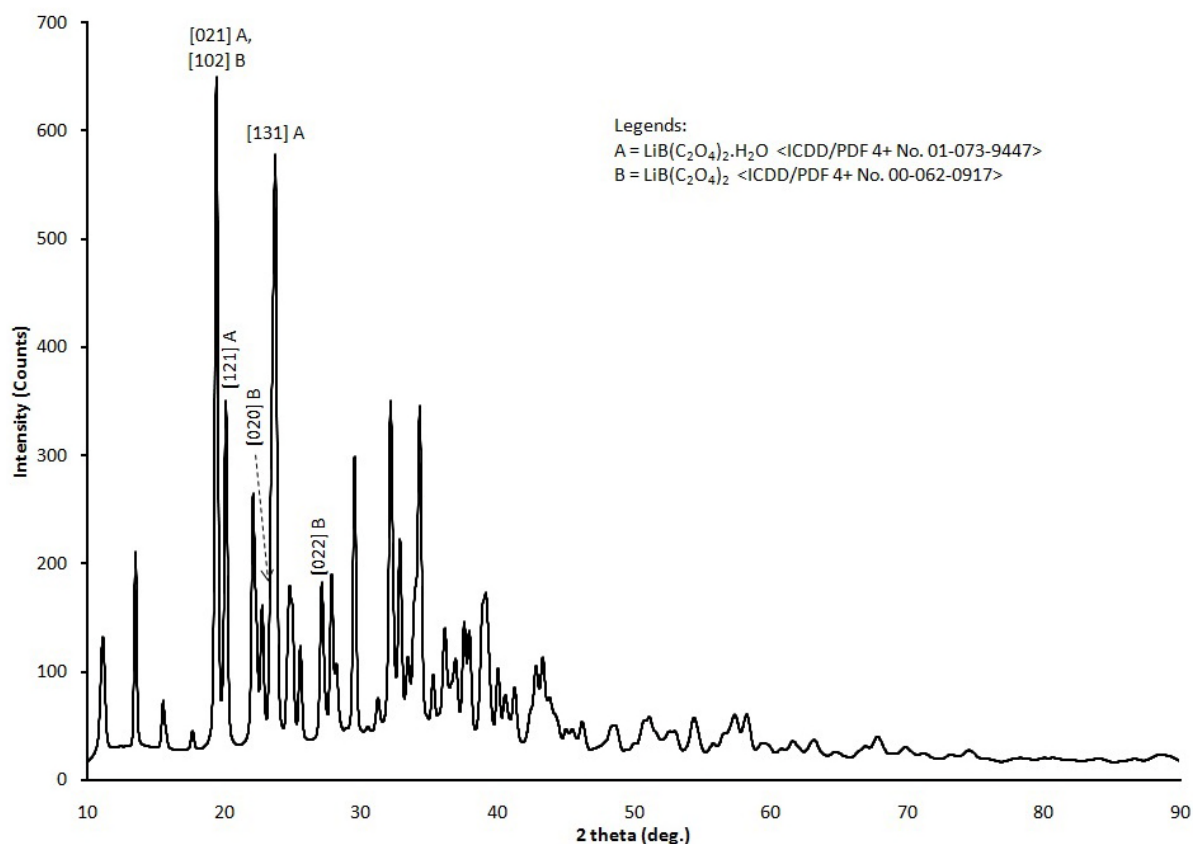


Fig 1. X-ray diffraction pattern of LiBOB powder

Table 1. Qualitative analysis result of LiBOB powder

Phase	Lattice Parameter			Crystal Structure	Space Group	Crystal Volume ( $\text{\AA}^3$ )	Density ( $\text{g/cm}^3$ )
	A ( $\text{\AA}$ )	B ( $\text{\AA}$ )	C ( $\text{\AA}$ )				
$\text{LiB}(\text{C}_2\text{O}_4)_2 \cdot \text{H}_2\text{O}$	16.1409	15.9370	5.6237	Orthorhombic	Pbca	1446.6	1.950
$\text{C}_4\text{LiBO}_8$	6.3719	7.6065	13.1800	Orthorhombic	Pnma	638.8	2.023

Table 2. Crystallite size calculation result

$2\theta$ (deg)	D ( $\text{\AA}$ )	FWHM (deg)	Crystallite Size (nm)
19.42	4.5669	0.236	35.7
20.13	4.4077	0.282	29.9
23.75	3.7437	0.415	20.4
32.15	2.7817	0.350	24.7

strongest lines of d-spacing value that was recorded in ICDD database. To determine a phase, three d-spacing values that was found from observation data with three strongest lines values were matched with ICDD database of the predicted phase. The matching tolerances are  $\pm 0.01$  for first d-spacing value and  $\pm 0.02$  for second and third d-spacing values. From the X-ray diffraction pattern of this sample, it was indicated that there were two main phases i.e.  $\text{LiB}(\text{C}_2\text{O}_4)_2 \cdot \text{H}_2\text{O}$  (LiBOB hydrate) and  $\text{C}_4\text{LiBO}_8$  (LiBOB). The LiBOB hydrate phase was indicated by three d-spacing values i.e. 3.74116  $\text{\AA}$ , 4.40427  $\text{\AA}$ , and 4.563  $\text{\AA}$  at 2-theta 23.7641 $^\circ$ , 20.1454 $^\circ$ , and 19.438 $^\circ$  that matched with ICDD/PDF 4+

database for LiBOB hydrate no. 01-073-9447 which had three strongest lines values i.e. 3.74141  $\text{\AA}$ , 4.41409  $\text{\AA}$ , and 4.57673  $\text{\AA}$ . The Miller indexes of these three strongest lines were [131], [121], and [021]. On the other hand, The LiBOB phase was indicated by three d-spacing values i.e. 4.563  $\text{\AA}$ , 3.78786  $\text{\AA}$ , and 3.27829  $\text{\AA}$  at 2-theta 19.438 $^\circ$ , 23.4669 $^\circ$ , and 27.1796 $^\circ$  that matched with ICDD/PDF 4+ database for LiBOB no. 00-062-0917 which had three strongest lines values i.e. 4.57621  $\text{\AA}$ , 3.79991  $\text{\AA}$ , and 3.29133  $\text{\AA}$ . The Miller indexes of these three strongest lines were [102], [020], and [022]. The qualitative analysis result of LiBOB powder sample was shown in Table 1.

The average crystallite size was determined from four highest intensities. The crystallite sizes of four maximum intensities were shown on Table 2. Based on full-width at half maximum (FWHM) value obtained from X-ray diffraction pattern, it was found that the average crystallite size was 25.175 nm with proximity of maximum size 35.7 nm and minimum size 20.4 nm.

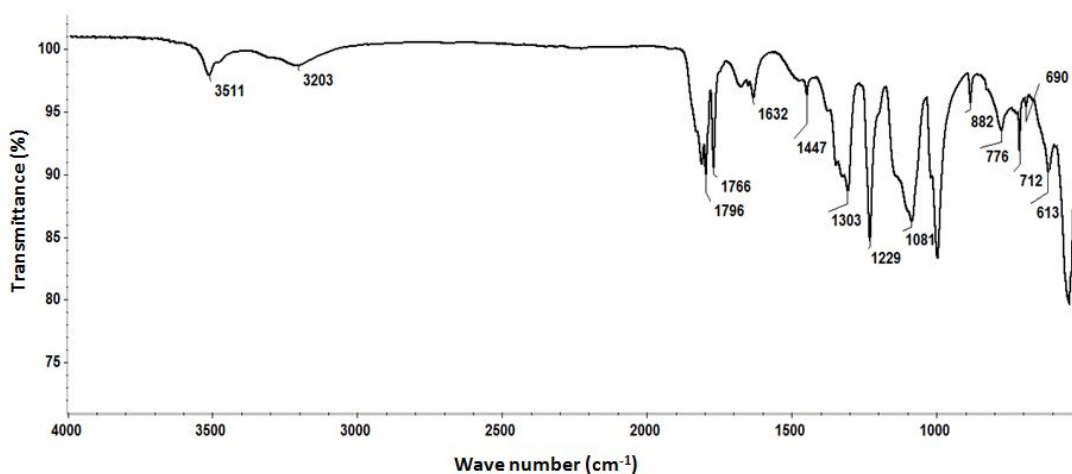


Fig 2. FT-IR spectrum of LiBOB powder

Table 3. Infra-red absorption band assignments for LiBOB

Wave number (cm <sup>-1</sup> )	Wave number ref[12] (cm <sup>-1</sup> )	Assignment
3512	-	O-H
3207	-	O-H
1808	1811	C=O Oscillate in phase
1796	1779	C=O Oscillate out of phase
1768	1750	C=O stretch
1633	1640	COO asymmetric stretch
1447	1442	C-H stretch
-	1372	B-O stretch
1303	1297	C-O-B-O-C stretch
1228	1215	C-O-C asymmetric stretch
1081	1070	O-B-O asymmetric stretch
-	1008	C-O-C asymmetric stretch
994	999	O-B-O asymmetric stretch
882	982	O-B-O asymmetric stretch
775	708	COO deform
613	604	B-O4 deform

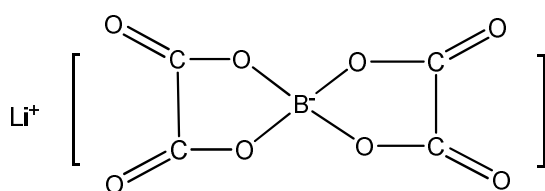


Fig 3. Structural formula of LiBOB compound

phase was found smaller than  $\text{LiB}(\text{C}_2\text{O}_4)_2 \cdot \text{H}_2\text{O}$ , because of the  $\text{H}_2\text{O}$  molecules inside  $\text{C}_4\text{LiBO}_8$ . On the other hand, the crystal density of  $\text{C}_4\text{LiBO}_8$  was found higher than  $\text{LiB}(\text{C}_2\text{O}_4)_2 \cdot \text{H}_2\text{O}$ , which means  $\text{C}_4\text{LiBO}_8$  was more dense.

### FT-IR Analysis

From the infrared spectrum shown in Fig. 2, it was seen that there were vibration probability of functional groups C-O, C=O, B-O, O-B-O and C-C in LiBOB powder following the structural formula that presented in Fig. 3. Wave number 1768–1808  $\text{cm}^{-1}$  and 994–1303  $\text{cm}^{-1}$  were assigned to C=O and C-O-B-O-C vibration, respectively. Wavenumber 775  $\text{cm}^{-1}$  was a typical C-O-O deform peak.

According to Aravindan and Vickraman [12], the absorption bands that must appear for LiBOB compound are at wave number 1372, 1087, and 860  $\text{cm}^{-1}$ , as shown at Table 3. It was also suggested

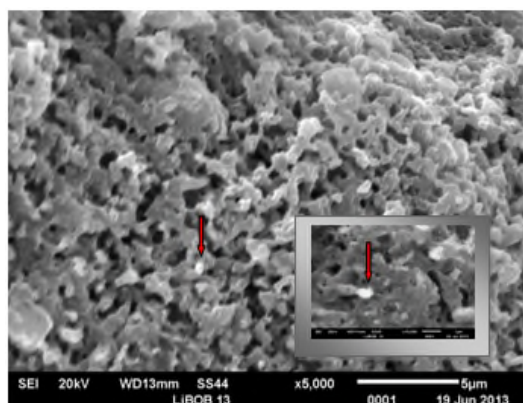


**Fig 4.** SEM figure of LiBOB powder at 5000x magnification, zoomed to 15,000x

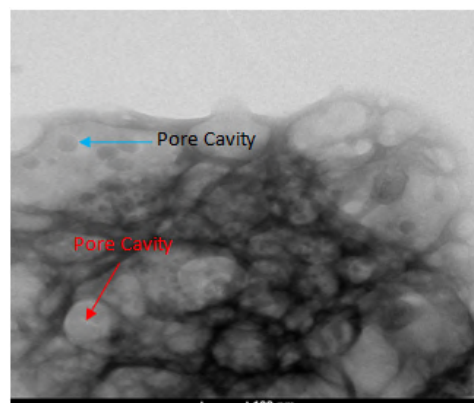


**Fig 5.** TEM image of synthesized LiBOB powder

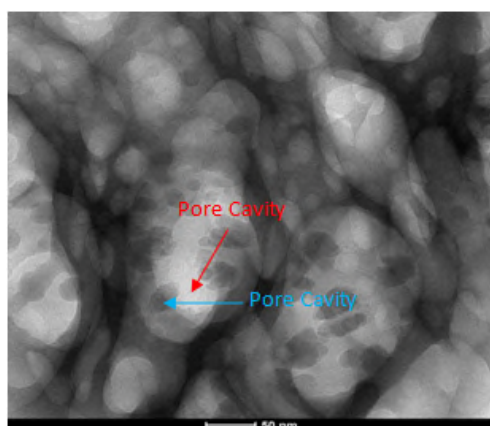


**Fig 6.** TEM image of commercial LiBOB powder

that C=O and B-O symmetric stretch at wave number 1750 and 1372  $\text{cm}^{-1}$  as well as asymmetric stretch of C-O-C at wave number 1008  $\text{cm}^{-1}$  did not appear for synthesized LiBOB. The absorption band O-B-O asymmetric stretch was observed at wave number 1081  $\text{cm}^{-1}$ , which was one of typical vibration peak of LiBOB compound. In reference LiBOB, this functional group was also identified at wave number 1070  $\text{cm}^{-1}$ .

Absorption bands appeared at wave number 3511 and 3412  $\text{cm}^{-1}$  were assigned for O-H bond. This bond indicates that there was probability of unfinished reaction of the boric acid or oxalic acid compound to produce LiBOB. It can also indicate that there was hydroxyl group from the moisture in the air attached to the newly-formed LiBOB molecules due to the hygroscopic nature of LiBOB. This attachment turned LiBOB phase into LiBOB hydrate phase, as was confirmed by the XRD analysis results.

### Surface Morphology

SEM image of LiBOB powder with 5,000x magnification shown at Fig. 4 showed that the powder

was in a form of hollow particle with irregular pores in micrometers size. The inset figure with 15,000x magnification showed that the darker shade was pore cavities with various size (approximately within 0.5–1  $\mu\text{m}$  range of diameter) among the particle bulges (the brighter shade). The pore cavities of LiBOB powder were distributed evenly on the entire surface. To observe the pore cavities of the sample more closely, TEM characterization was conducted; the result is presented at Fig. 5.

It was observed that the pores were in elongated, round shape. TEM image at Fig. 5 showed that the brighter shade was the pore cavities surrounded by the darker shade in a single LiBOB particle. Another pore was seen inside the pore cavities, which implies that there are many pores inside one single particle with pore size of 50–100 nm range. TEM analysis of commercial LiBOB powder (Sigma Aldrich) was presented at Fig. 6. There was also pore inside the pore cavities, shown in darker shade with 25–50 nm size, and spread evenly.

This phenomenon has shown that the synthesis of LiBOB in this study has resulted in LiBOB powder with nanopores structure. Nanopores formation in the LiBOB powder was due to the chemical reaction between the raw materials, i.e. lithium hydroxide, oxalic acid and boric acid to form LiBOB and removing water molecules. During the heat treatment process, the water molecules evaporated and left empty spaces in the form of micro and nanopores. Nanopores structure is highly required in the properties of electrolyte active material to increase solubility in the synthesis of liquid electrolyte, because the solvent would be easily immersed into the porous particle and dissolve it. The nano-sized pores is also advantageous for the particle, for the increase of total pore surface will be also increasing particle solubility. From the commercial LiBOB observation it was also seen the evenly distributed nano-sized pores. It could be concluded that

the microstructure of synthesized LiBOB has similarity in qualities and features with commercial LiBOB.

### Surface Area

Surface area analysis using Quantachrome Nova 4200e resulted in LiBOB powder surface area, total pore volume, and average pore diameter of 88.556 m<sup>2</sup>/g, 0.4252 cm<sup>3</sup>/g, and 19.2 nm, respectively. In the experiment, LiBOB synthesis produced a powder with large enough surface area to accommodate contact between LiBOB particle and carbonate solvents in liquid electrolyte system. The larger the surface areas of a particle, more particles are exposed and the numbers of total collisions are increased, hence increasing the reaction rate. Therefore, with large surface area LiBOB powder is expected to be easily soluble in carbonate solvents.

It was seen that pore size analysis using BET method was smaller, micropore size category, than using TEM, because the result from TEM analysis was obtained visually using the image of the sample being observed while the result from BET method was obtained theoretically from gas adsorption on the sample surface.

### CONCLUSION

Microstructure observation of LiBOB was important in synthesizing liquid electrolyte for lithium-ion batteries application. Several parameters, such as particle size, particle morphology and the degree of crystallinity should be observed as well. In this research, synthesized LiBOB has been observed by using XRD, BET, SEM, and TEM to show its crystalline structure and particle morphology. In this microstructure analysis, it was observed that there were two phases: LiBOB and LiB(C<sub>2</sub>O<sub>4</sub>)<sub>2</sub>·H<sub>2</sub>O. LiBOB phase has orthorhombic crystal structure. Particle morphology analysis using SEM has shown that there are pore cavities inside the particle. From TEM analysis, it can also be seen that synthesis of LiBOB by means of solid state reaction resulted in

particle with nanopore structure, with pore size of 50–100 nm. Surface area analysis using BET has calculated LiBOB powder surface area, total pore volume, and average pore diameter of 88.556 m<sup>2</sup>/g, 0.4252 cm<sup>3</sup>/g, and 19.2 nm, respectively.

### ACKNOWLEDGEMENT

This work was supported by Research Center for Physics Department, Indonesian Institute of Sciences through DIPA program budget year of 2014, No 3401.001.001.011.

### REFERENCES

1. Lischka, U., Wietelmann, U., and Wegner, M., 1999, German Pat., DE 19829030C1.
2. Xu, W., and Angel, C.A., 2001, *Electrochem. Solid-State Lett.*, 4 (1), E1–E4.
3. Cui, X., Zhang, H., Li, S., Li, X., and Feng, H., 2014, *Ionics*, 20 (6), 789–794.
4. Barth, W.V., Hueso, A.P., Zhou, L., Lyons, L.J., and West, R., 2014, *J. Power Sources*, 272, 190–195.
5. Fan, L.Z., Xing, T., Awan, R., and Qiu, W., 2011, *Ionics*, 17 (6), 491–494.
6. Yu, Z., Xu, T., Xing, T., Fan, L.-Z., Lian, F., and Qiu, W., 2010, *J. Power Sources*, 195 (13), 4285–4289.
7. Kaneko, H., Sekine, K., and Takamura, T., 2005, *J. Power Sources*, 146 (1-2), 142–145.
8. Wang, S., Qiu, W., Guan, Y., Yu, B., Zhao, H., and Liu, W., 2007, *Electrochim. Acta*, 52 (15), 4907–4910.
9. Yu, B., Qiu, W., Li, F., and Xu, G., 2006, *Electrochem. Solid-State Lett.*, 9 (1), A1–A4.
10. Rahaman, M.H.A., Khandaker, M.U., Khan, Z.R., Kufian, M.Z., Noor, I.S.M., and Arof, A.K., 2014, *Phys. Chem. Chem. Phys.*, 16 (23), 11527–11537.
11. Moryc, U., and Ptak, W.S., 1999, *J. Mol. Struct.*, 511-512, 241–249.
12. Aravindan, V., and Vickraman, P., 2007, *Ionics*, 13 (4), 277–280.